⌘ *Author's Choice*

Uncoupling Protein 3 (UCP3) Modulates the Activity of Sarco/Endoplasmic Reticulum Ca²⁺-ATPase (SERCA) by Decreasing Mitochondrial ATP Production*⑤

Umberto De Marchi, Cyril Castelbou, and Nicolas Demaurex[1]
From the Department of Cell Physiology and Metabolism, University of Geneva, rue Michel-Servet, 1, CH-1211 Genève, Switzerland

The uncoupling proteins UCP2 and UCP3 have been postulated to catalyze Ca²⁺ entry across the inner membrane of mitochondria, but this proposal is disputed, and other, unrelated proteins have since been identified as the mitochondrial Ca²⁺ uniporter. To clarify the role of UCPs in mitochondrial Ca²⁺ handling, we down-regulated the expression of the only uncoupling protein of HeLa cells, UCP3, and measured Ca²⁺ and ATP levels in the cytosol and in organelles with genetically encoded probes. UCP3 silencing did not alter mitochondrial Ca²⁺ uptake in permeabilized cells. In intact cells, however, UCP3 depletion increased mitochondrial ATP production and strongly reduced the cytosolic and mitochondrial Ca²⁺ elevations evoked by histamine. The reduced Ca²⁺ elevations were due to inhibition of store-operated Ca²⁺ entry and reduced depletion of endoplasmic reticulum (ER) Ca²⁺ stores. UCP3 depletion accelerated the ER Ca²⁺ refilling kinetics, indicating that the activity of sarco/endoplasmic reticulum Ca²⁺ (SERCA) pumps was increased. Accordingly, SERCA inhibitors reversed the effects of UCP3 depletion on cytosolic, ER, and mitochondrial Ca²⁺ responses. Our results indicate that UCP3 is not a mitochondrial Ca²⁺ uniporter and that it instead negatively modulates the activity of SERCA by limiting mitochondrial ATP production. The effects of UCP3 on mitochondrial Ca²⁺ thus reflect metabolic alterations that impact on cellular Ca²⁺ homeostasis. The sensitivity of SERCA to mitochondrial ATP production suggests that mitochondria control the local ATP availability at ER Ca²⁺ uptake and release sites.

Mitochondria are multifunctional organelles that control the life and death of cells. Mitochondria are the site of oxidative phosphorylation and convert reducing equivalents into the ATP that cells use as energy source, release critical factors that induce the programmed cell death of apoptosis, and modulate cell signaling by capturing and subsequently releasing calcium ions. The ability of mitochondria to sequester Ca²⁺ ions released from the endoplasmic reticulum or entering across plasma membrane channels enables these organelles to shape cytosolic Ca²⁺ signals and to modulate the activity of membrane channels and transporters (1–3), whereas Ca²⁺ elevations within the matrix of mitochondria activate three enzymes of the tricarboxylic cycle, thereby boosting oxidative phosphorylation and ATP production. Calcium uptake and release by mitochondria are therefore essential for the patterning of cytosolic Ca²⁺ signals and for cells to decode Ca²⁺ signals as either metabolic or death signals. The importance of mitochondrial Ca²⁺ handling for cell physiology has fostered a long quest to identify the transport molecules that move Ca²⁺ in and out of mitochondria (4). This quest culminated in recent years with the report of several families of proteins that were proposed to participate in either mitochondrial Ca²⁺ uptake or mitochondrial Ca²⁺ extrusion: the uncoupling proteins 2 and 3 (UCP2 [2] and UCP3), the leucine zipper EF-hand-containing transmembrane protein 1 (Letm1), the Na⁺/Ca²⁺ exchanger (NCLX), the stomatin-like protein 2 (SLP-2), and the mitochondrial calcium uptake protein 1 (MICU1).

Ca²⁺ enters mitochondria across a mitochondrial Ca²⁺ uniporter (MCU) that was characterized in 2004 at the electrophysiological level as a highly selective inward rectifying mitochondrial inner membrane Ca²⁺ channel, inhibited by ruthenium red and Ru360 (5). In 2007, UCP2 and UCP3 were proposed to be fundamental for the MCU (6), based on the altered mitochondrial Ca²⁺ elevations ($[Ca^{2+}]_{mit}$) of cells enriched or depleted of UCP2 or UCP3 and on the defective ruthenium red-sensitive Ca²⁺ uptake of liver mitochondria isolated from UCP2⁻/⁻ mice. This proposal was subsequently refuted by a study showing that purified liver mitochondria from UCP2⁻/⁻ and UCP3⁻/⁻ mice take up calcium normally (7). In 2009, Letm1, a protein previously shown to catalyze mitochondrial K⁺/H⁺ exchange (8, 9), was shown to drive mitochondrial Ca²⁺ uptake by exchanging Ca²⁺ for H⁺ with a 1:1 stoichiometry (10). This stoichiometry, however, contradicts earlier studies in isolated mitochondria showing that Ca²⁺ enters mitochondria together with two positive charges and leaves the matrix in exchange for three protons (reviewed in Ref. 4). Letm1 is associated with Wolf-Hirschhorn syndrome, a severe human neurological disease characterized by mental retardation and seizures (11). In 2010, MICU1, an inner mito-

---

[1] To whom correspondence should be addressed. Tel.: 41-22-379-5399; Fax: 41-22-379-5338; E-mail: Nicolas.Demaurex@unige.ch.

[2] The abbreviations used are: UCP, uncoupling protein; ER, endoplasmic reticulum; SERCA, sarco/endoplasmic reticulum Ca²⁺ -ATPase; MCU, mitochondrial Ca²⁺ uniporter; SOCE, store-operated Ca²⁺ entry; BHQ, 2,5-di-*t*-butyl-1,4-benzohydroquinone; $[Ca^{2+}]_{cyto}$, cytosolic $[Ca^{2+}]$; $[Ca^{2+}]_{ER}$, endoplasmic reticulum $[Ca^{2+}]$; $[Ca^{2+}]_{mit}$, mitochondrial $[Ca^{2+}]$; TG, thapsigargin; YC, yellow cameleon; Ctrl, control; HEDTA, *N*-(2-hydroxyethyl)ethylenediaminetriacetic acid.

chondrial membrane protein with two Ca^{2+}-binding EF-hand domains, was shown to be required for high capacity mitochondrial calcium uptake (12). MICU1 is a single-pass transmembrane protein unlikely to form a channel pore and was proposed to be the calcium sensing regulatory subunit of the MCU because mutations of its EF-hand domains abrogate mitochondrial Ca^{2+} uptake (13). Two proteins were reported to modulate Ca^{2+} extrusion from mitochondria. NCLX/NCKX6 was shown to catalyze CGP-37157-sensitive mitochondrial Na^+/Ca^{2+} exchange (14), and SLP-2 was shown to negatively modulate the activity of the mitochondrial sodium-calcium exchanger (15).

The successive reports of proteins essential for mitochondrial Ca^{2+} uptake have generated some confusion about the identity and mode of operation of the MCU. The first proteins proposed to be fundamental for the MCU, UCP2 and UCP3 (16), are mitochondrial inner membrane protein paralogues of UCP1, the first UCP cloned. UCP1 is almost exclusively expressed in brown adipose tissue, where it catalyzes adaptive thermogenesis by acting as a mitochondrial proton channel, thereby uncoupling oxidative phosphorylation from ATP synthesis (17). Unlike UCP1, UCP2 and UCP3 are expressed in several tissues and are present in ectothermic fishes and plants that do not require thermogenesis. The basal H^+ conductance is unchanged in mitochondria isolated from UCP2 or UCP3 null mice (18, 19), and the novel UCP homologues have been proposed to mediate regulated proton leak (20), to modulate insulin secretion (21), and to regulate the export of fatty acids and fatty acid peroxides(22, 23). The ability of UCP2/3 to act as proton leak channels seems strictly related to the presence of specific activators such as alkenyls produced by the peroxidation of membrane phospholipids (24, 25). Thus, there is a broad consensus that UCP2 and UCP3 do not mediate adaptive thermogenesis (25–27). Instead, the novel UCPs might act as mild uncouplers and protect against oxidative damage by attenuating the mitochondrial production of free radicals (28, 29).

The report that the amplitude of $[Ca^{2+}]_{mit}$ elevations in intact cells directly correlates to the expression level of UCP2 and UCP3 (6) might explain the plethoric effects attributed to UCPs because alterations in $[Ca^{2+}]_{mit}$ signals are expected to impact both on mitochondria bioenergetics and on cell signaling. Whether the altered $[Ca^{2+}]_{mit}$ signals are due to defective mitochondrial Ca^{2+} uptake is unclear due to the conflicting reports obtained in isolated liver mitochondria from UCP2$^{-/-}$ null mice (6, 7). These opposite datasets could be reconciled by postulating a regulatory role for UCP2 and UCP3 in intact cells that would be lost in isolated mitochondria. Importantly, the altered $[Ca^{2+}]_{mit}$ signals reported by Trenker *et al.* (6) in intact cells depleted or enriched of UCP2/3 have not been confirmed or disproved. To clarify the physiological role of UCPs in Ca^{2+} homeostasis, we used RNA interference to down-regulate UCP3, the only UCP isoform of HeLa cells (6), and measured the impact of UCP3 depletion on the Ca^{2+} and ATP levels in different cellular compartments.

EXPERIMENTAL PROCEDURES

Reagents—Minimal essential medium, fetal calf serum, penicillin, streptomycin, and Lipofectamine 2000 transfection rea-

gent were obtained from Invitrogen. Histamine, thapsigargin (TG), antimycin A, and oligomycin were obtained from Sigma. 2,5-Di-*t*-butyl-1,4-benzohydroquinone (BHQ) were from Aldrich. Fura-2 AM was from Molecular Probes. YC3.6$_{cyto}$ (30), 4mtD3cpv (31), and D1$_{ER}$ (32) constructs were kindly provided by Drs. Amy Palmer and Roger Tsien (University of California, San Diego). Mitochondrial and cytosolic FRET-based ATP indicators (ATeam: adenosine 5′-triphosphate indicator based on the ϵ subunit for Analytical Measurements) were kindly provided by Drs. Hiromi Imamura (Japan Science and Technology Agency, Tokyo) and Hiroyuki Noji (Osaka University) (33). UCP2 and UCP3/mitochondria-targeted DsRed constructs were kindly provided by Dr. Wolfgang Graier (Medical University of Graz).

Cell Culture, Transfection, and RNA Interference—Culturing of HeLa cells has been previously described (34). For all experiments, cells were plated on 25-mm-diameter glass coverslips and co-transfected with the plasmid (1 μg/ml) coding for Ca^{2+} or pH probe and dsRNA using Lipofectamine 2000. All experiments were performed 2 days after transfection. For silencing UCP3 expression, commercial double-stranded RNAs from Qiagen were used (Hi PerFect-validated siRNA S102780771). For controls, cells were transfected with nonsilencing siRNA (AllStars negative control siRNA, Qiagen 1027281). Knockdown efficiency was verified by Western blots.

Cell Lysis, Mitochondrial Isolation, and Western Blotting—Whole cells were lysed for 30 min on ice in lysis buffer (25 mM Tris-HCl, pH 7.6, 150 mM NaCl, 1% Nonidet P-40, 1% sodium deoxycholate, 0.1% SDS) supplemented with protease inhibitors (Roche Applied Science). The lysate was centrifuged at $14,000 \times g$ for 20 min, and the protein content of the supernatant was determined using the BCA protein assay (Pierce). The mitochondrial fraction was obtained by differential centrifugation as reported previously (35). 50 μg of total protein (from cell lysate or isolated mitochondria) was loaded per lane of SDS-PAGE. For immunoblotting, proteins were transferred onto nitrocellulose membrane and probed with the following antibodies: anti-UCP3 (Santa Cruz Biotechnology, sc-7756) and anti-Tom20 (Santa Cruz Biotechnology, sc-11415), anti-SERCA2 (Thermo Scientific MA3-919), and anti-actin (Chemicon). Horseradish peroxidase-conjugated secondary antibodies (Amersham Biosciences) were used followed by detection by chemiluminescence (Amersham Biosciences).

Mitochondrial, Cytosolic, and Endoplasmic Reticulum Ca^{2+} Measurements—Experiments were performed in HEPES buffer solution containing (in mM): 140 NaCl, 5 KCl, 1 MgCl$_2$, 2 CaCl$_2$, 20 Hepes, 10 glucose, pH 7.4, with NaOH at 37 °C. Ca^{2+}-free solution contained 1 mM EGTA instead of CaCl$_2$. Glass coverslips were inserted in a thermostatic chamber (Harvard Apparatus, Holliston, MA), and solutions were changed by hand. Cells were imaged on an Axiovert s100 TV using a ×40, 1.3 NA oil immersion objective (Carl Zeiss AG, Feldbach, Switzerland) and a cooled, 16-bit CCD back-illuminated frame transfer MicroMax camera (Roper Scientific, Trenton, NJ). Cytosolic Ca^{2+} was measured with fura-2 (2 μM, 0.2% dimethyl sulfoxide (DMSO), 0.01% Pluronic F127, Invitrogen) followed by 20 min of de-esterification before 10 min of equilibration on the heated stage or with YC3.6$_{cyto}$. Mitochondrial and endoplasmic retic-

ulum Ca^{2+} levels were measured with 4mtD3cpv and $D1_{ER}$, respectively. For dual emission imaging of cameleon constructs (4mtD3cpv, $YC3.6_{cyto}$, and $D1_{ER}$), cells were excited at 430 nm through a 455DRLP dichroic and alternately imaged with 480AF30 and 535DF25 emission filters (Omega Optical). Fura-2 was measured simultaneously with 4mtD3cpv and was excited alternately at 340 and 380 nm through a 455DRLP dichroic and 535DF25 emission filter. Images were acquired every 2 s. Fluorescence ratios were calculated in MetaFluor 6.3 (Universal Imaging) and analyzed in Excel (Microsoft) and GraphPad Prism 4 (GraphPad). $[Ca]_{ER}$ was calculated from $D1_{ER}$ ratios using the equation

$$R = R_{min} + \frac{[R_{max} - R_{min}]}{1 + 10^{(Log K'_d - Log[Ca^{2+}]_{ER})h}} \qquad \text{(Eq. 1)}$$

where R_{min} and R_{max} are the minimal and maximal ratio obtained at $pCa > 8$ and < 2, respectively, K'_d is the apparent dissociation constant, and h is the Hill coefficient derived from the *in situ* Ca^{2+} titration of the $D1_{ER}$ probe in semipermeabilized cells, as described previously (36).

Mitochondrial and Cytosolic [ATP] Measurements—ATP imaging was performed on the epifluorescence system described above, with the genetically encoded ATP sensors $ATeam_{mito}$ and $ATeam_{cyto}$, for mitochondrial and cytosolic ATP, respectively. For the dual emission imaging of these two cameleon-based constructs, cells were excited and imaged as described previously for mitochondrial Ca^{2+} imaging. Images were acquired every 2 s. Fluorescence ratios were normalized on the minimum of fluorescence (R_{min}), obtained after inhibition of glycolysis with 10 mM 2-deoxyglucose and in the presence of the inhibitor of mitochondrial ATP synthesis oligomycin A (10 μg/ml). Data were analyzed as described previously.

Permeabilized Cells—Cells were washed with high K^+ intracellular buffer, containing (in mM) 110 KCl, 10 NaCl, 0.5 K_2HPO_4, 5 succinate, 10 mM HEPES (pH 7.0 at 37 °C), supplemented with 5 HEDTA or 1 EGTA. For permeabilization, 100 μM digitonin was added for 1 min, and the cells were then allowed to recover in intracellular buffer before the addition of $CaCl_2$. Free $[Ca^{2+}]$ was calculated with the Maxchelator program.

Statistics—The significance of differences between means was established using the Student's *t* test for unpaired samples (*, $p < 0.05$; **, $p < 0.01$; ***, $p < 0.001$).

RESULTS

Effect of UCP3 Depletion on Mitochondrial and Cytosolic Ca^{2+} Elevations—To clarify the role of UCPs in mitochondrial Ca^{2+} handling, we measured Ca^{2+} responses in the cytosol and in mitochondria in HeLa cells depleted or not of UCP3, the only novel UCP isoform expressed in this cell type (6). Consistent with earlier results (6), this treatment decreased UCP3 protein levels by 50% (supplemental Fig. S1). Cells were then transfected with a cameleon Ca^{2+} probe targeted to mitochondria (Fig. 1*A*) or to the cytosol (Fig. 1*B*) to enable $[Ca^{2+}]_{mit}$ and $[Ca^{2+}]_{cyt}$ recordings. As shown in Fig. 1*A*, UCP3 depletion strongly reduced the $[Ca^{2+}]_{mit}$ elevations evoked by histamine, the peak $[Ca^{2+}]_{mit}$ response being reduced by 57% and the inte-

○ Control siRNA ● UCP3 siRNA
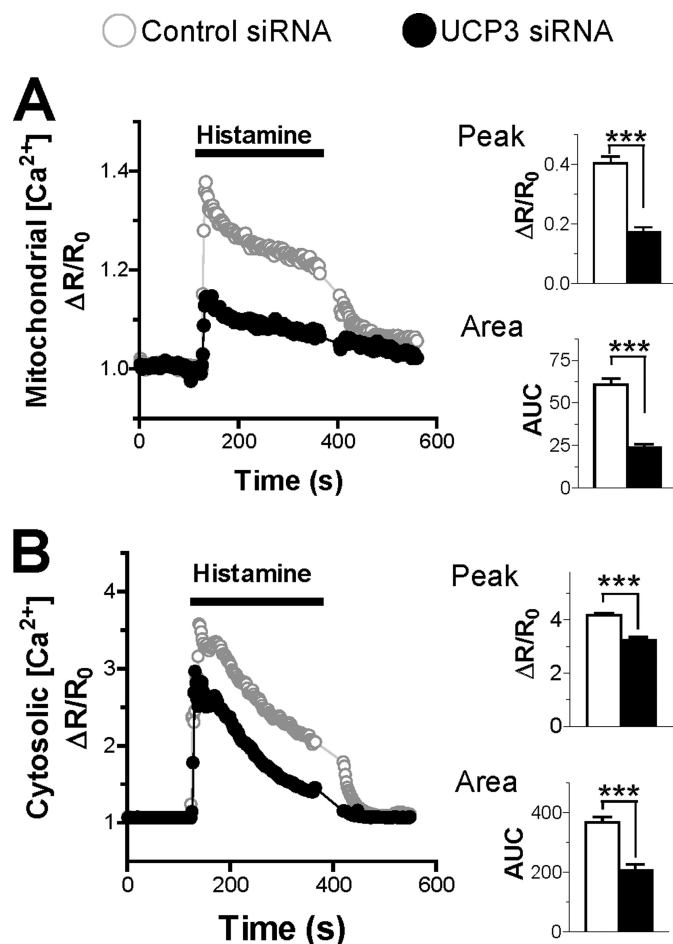
FIGURE 1. **Effect of UCP3 knockdown on mitochondrial and cytosolic Ca^{2+} elevations.** *A* and *B*, HeLa cells were transiently co-transfected with the mitochondrial Ca^{2+} probe 4mtD3cpv (*A*) or the cytosolic Ca^{2+} probe $YC3.6_{cyto}$ (*B*) and with either scrambled siRNA (*control siRNA*) or UCP3-specific siRNA (*UCP3 siRNA*) for 48 h. *A, left,* averaged $[Ca^{2+}]_{mit}$ recordings in HeLa cells stimulated with 100 μM histamine. *Right,* statistical evaluation of the UCP3 siRNA effects on the amplitude of the $[Ca^{2+}]_{mit}$ signal evoked by histamine (*upper panel*) and on the integrated $[Ca^{2+}]_{mit}$ response (*lower panel*). *Bars* are mean $\pm$ S.E. of 80 ($n = 7$) and 101 cells ($n = 7$) for Ctrl and UCP3 siRNA, respectively. *AUC*, area under the curve. *B, left,* averaged $[Ca^{2+}]_{cyto}$ recordings in HeLa cells stimulated with 100 μM histamine. *Right,* statistical evaluation of the UCP3 siRNA effects on the amplitude of the $[Ca^{2+}]_{cyto}$ signal evoked by histamine (*upper panel*) and on the integrated $[Ca^{2+}]_{cyto}$ response (*lower panel*). *Bars* are mean $\pm$ S.E. of 40 ($n = 3$) and 37 cells ($n = 3$) for Ctrl and UCP3 siRNA, respectively. ***, $p < 0.001$.

grated response being reduced by 62%. To exclude possible off-target effects linked to siRNA transfection, we overexpressed UCP3 protein and, in another set of experiments, attempted to rescue the defect caused by UCP3 siRNA by expressing another uncoupling protein, UCP2. As shown in supplemental Fig. S2A, UCP3 overexpression significantly increased the peak and integrated $[Ca^{2+}]_{mit}$ responses evoked by histamine, mirroring the effects of UCP3 depletion, whereas expression of UCP2 restored normal $[Ca^{2+}]_{mit}$ responses in cells depleted of UCP3 (supplemental Fig. S3A). These data indicate that the altered mitochondrial Ca^{2+} signals are indeed causally related to the changes in UCP3 levels. The UCP3-dependent Ca^{2+} defect was not restricted to mitochondria, however, because the cytosolic Ca^{2+} elevations were also reduced in cells depleted of UCP3, the peak and integrated $[Ca^{2+}]_{cyt}$ responses being decreased by 25 and 44%, respectively (Fig. 1*B*). To confirm that the altera-
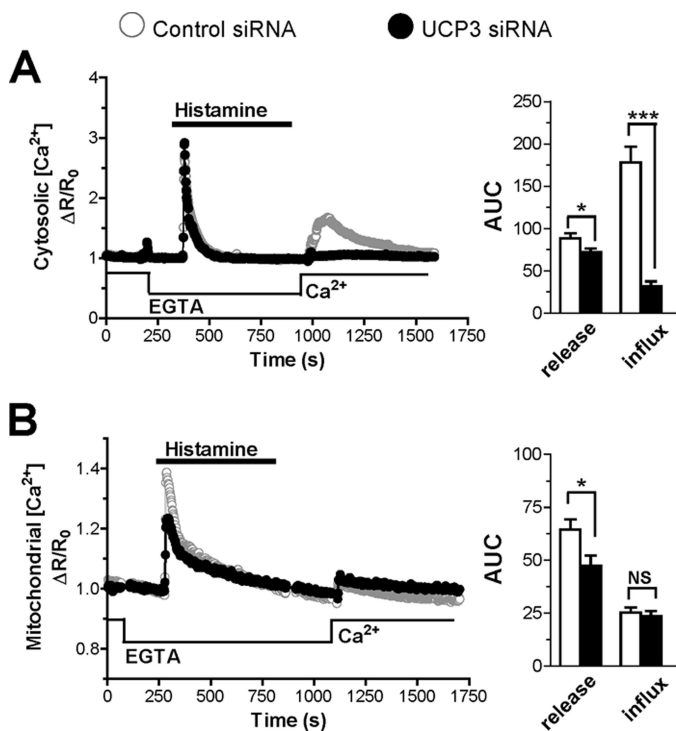
FIGURE 2. **Effect of UCP3 knockdown on Ca^{2+} release and influx.** *A* and *B*, HeLa cells were transiently co-transfected with the cytosolic Ca^{2+} probe $YC3.6_{cyto}$ (*A*) or the mitochondrial Ca^{2+} probe 4mtD3cpv (*B*) and with Ctrl (scramble) siRNA or the UCP3 siRNA for 48 h, washed, and stimulated with 100 μM histamine in Ca^{2+}-free medium to deplete intracellular Ca^{2+} stores. Then Ca^{2+} was readmitted to monitor Ca^{2+} influx from plasma membrane. *A*, average of cytosolic Ca^{2+} responses (*left*) elicited by histamine and by Ca^{2+} readmission. *Right*, statistical evaluation of the UCP3 siRNA on the integrated $[Ca^{2+}]_{cyto}$ response during release from ER and during Ca^{2+} readmission. *Bars* are mean $\pm$ S.E. of 84 (*n* = 9) and 86 cells (*n* = 8) for Ctrl and UCP3 siRNA, respectively. *AUC*, area under the curve. *B*, average of mitochondrial Ca^{2+} responses elicited by histamine and Ca^{2+} readmission (*left*) and related statistical evaluation (*right*) on integrated $[Ca^{2+}]_{cyto}$ response during Ca^{2+} release and influx. *Bars* are mean $\pm$ S.E. of 77 (*n* = 8) and 59 cells (*n* = 7) for Ctrl and UCP3 siRNA, respectively. *, $p < 0.05$; ***, $p < 0.001$. *NS*, not significant.

tion in Ca^{2+} handling affected both compartments, we measured $[Ca^{2+}]_{cyt}$ and $[Ca^{2+}]_{mit}$ simultaneously instead of separately. In these conditions, both the cytosolic and the mitochondrial Ca^{2+} responses were blunted in cells depleted of UCP3 (supplemental Fig. S4). These data indicate that UCP3 knockdown has a global effect and not only blunts mitochondrial Ca^{2+} elevations but also reduces cytosolic Ca^{2+} elevations.

Effect of UCP3 Depletion on Agonist-evoked Ca^{2+} Release and Influx—The novel UCPs have been recently proposed to specifically mediate the mitochondrial uptake of Ca^{2+} released from the ER, but not of the Ca^{2+} entering across SOCE channels (37). To verify this possibility, we separated the agonist-evoked Ca^{2+} response into its release and influx components. Cells were stimulated with histamine in Ca^{2+}-free conditions to mobilize Ca^{2+} from stores, and Ca^{2+} was subsequently readmitted to promote Ca^{2+} entry. As shown in Fig. 2, the $[Ca^{2+}]_{cyt}$ and $[Ca^{2+}]_{mit}$ elevations caused by Ca^{2+} release from stores were slightly but significantly decreased. This inhibition, however, was much smaller than the inhibition observed in Ca^{2+}-containing medium (Fig. 1). Unexpectedly, the $[Ca^{2+}]_{cyt}$ elevations evoked by Ca^{2+} readmission were severely blunted in cells

depleted of UCP3, the integrated $[Ca^{2+}]_{cyt}$ response being reduced by 82% (Fig. 2*A*). An opposite effect was obtained by overexpressing UCP3, the $[Ca^{2+}]_{cyt}$ responses increasing slightly (14%) during Ca^{2+} release from stores and markedly (75%) during Ca^{2+} influx (supplemental Fig. S2*B*). Moreover, UCP2 expression restored a normal Ca^{2+} influx in UCP3-depleted cells (supplemental Fig. S3*B*), confirming that this defect was due to the depletion of an uncoupling protein. As reported previously (38), the $[Ca^{2+}]_{mit}$ elevations evoked by this Ca^{2+} readmission protocol were barely detectable and were not altered by UCP3 depletion (Fig. 2*B*).

These observations indicate that UCP3 depletion slightly impairs Ca^{2+} release from stores and, surprisingly, strongly inhibits the cytosolic Ca^{2+} elevations caused by Ca^{2+} readmission to cells with depleted Ca^{2+} stores. The primary effect of UCP3 depletion thus appears to be a reduced entry of Ca^{2+} across SOCE channels.
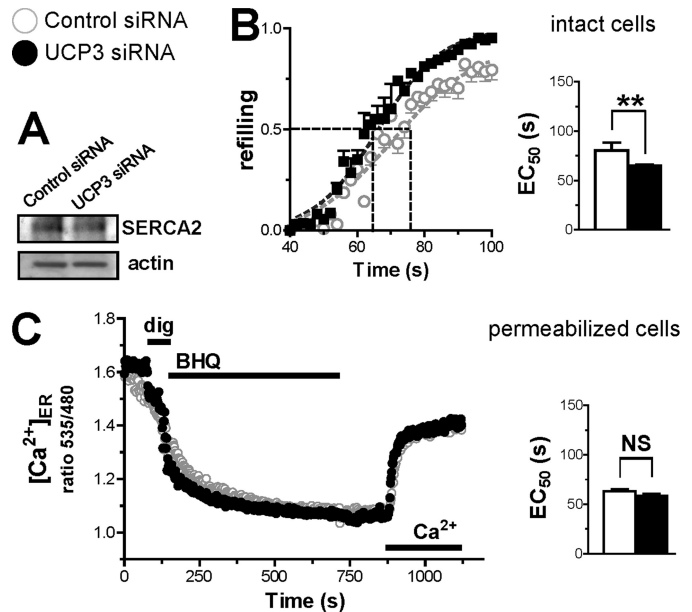
Effect of UCP3 Depletion on ER Ca^{2+} Release and Refilling—SOCE channels are activated by the depletion of ER Ca^{2+} stores, which induces the translocation of the ER-resident Ca^{2+} sensor STIM1 to the plasma membrane, where it binds and activates the Orai and Transient Receptor Potential channels (39). The reduced Ca^{2+} entry of UCP3 knockdown cells suggested that the SOCE machinery was inhibited, prompting us to study the filling state of ER Ca^{2+} stores. We therefore measured $[Ca^{2+}]_{ER}$ at rest and during store depletion with the ER-targeted cameleon Ca^{2+} indicator $D1_{ER}$. As shown in Fig. 3*A*, $D1_{ER}$ basal ratio fluorescence levels were identical in control and UCP3-depleted cells, the basal $[Ca^{2+}]_{ER}$ levels averaging 520 μM in both conditions (supplemental Fig. S5, *A* and *B*). Upon stimulation with histamine, however, $[Ca^{2+}]_{ER}$ decreased much more slowly in cells depleted of UCP3, the half-time increasing from 72 to 269 s (Fig. 3*B*, *inset*). This four times slower $[Ca^{2+}]_{ER}$ decrease was surprising considering that UCP3 knockdown cells released Ca^{2+} efficiently when stimulated with agonists (Fig. 2*A*). Reduced depletion of ER Ca^{2+} stores could reflect either a reduced passive permeability to Ca^{2+} or an increased Ca^{2+} pumping into the ER. To distinguish between these possibilities, we inhibited SERCA pumps with TG to reveal the intrinsic Ca^{2+} leak rates of the ER. As shown in Fig. 3*C*, the addition of TG elicited identical $[Ca^{2+}]_{ER}$ decreases in control and UCP3 knockdown cells, indicating that the passive Ca^{2+} permeability of the ER was not affected by the depletion of UCP3. The addition of TG together with histamine accelerated the kinetics of $[Ca^{2+}]_{ER}$ decrease by ~2-fold in UCP3-depleted cells, but these cells still released Ca^{2+} more slowly than control cells (supplemental Fig. S5*C*). Because $[Ca^{2+}]_{ER}$ decreased significantly ~40 s after TG addition (supplemental Fig. S5*D*), we then added TG 40 s before histamine to ensure full inhibition of SERCA. In these conditions, the kinetics of $[Ca^{2+}]_{ER}$ decrease evoked by histamine were similar in control and UCP3-depleted cells (Fig. 3*D*). These data indicate that the both the passive and the active (*i.e.* InsP3R-mediated) Ca^{2+} permeability of the ER are not affected by the depletion of UCP3. Similar effects were observed with the reversible SERCA inhibitor BHQ (not shown), confirming the involvement of SERCA. Of note, BHQ required more time than TG to completely inhibit SERCA pumps (supplemental Fig. S5*E*; see under
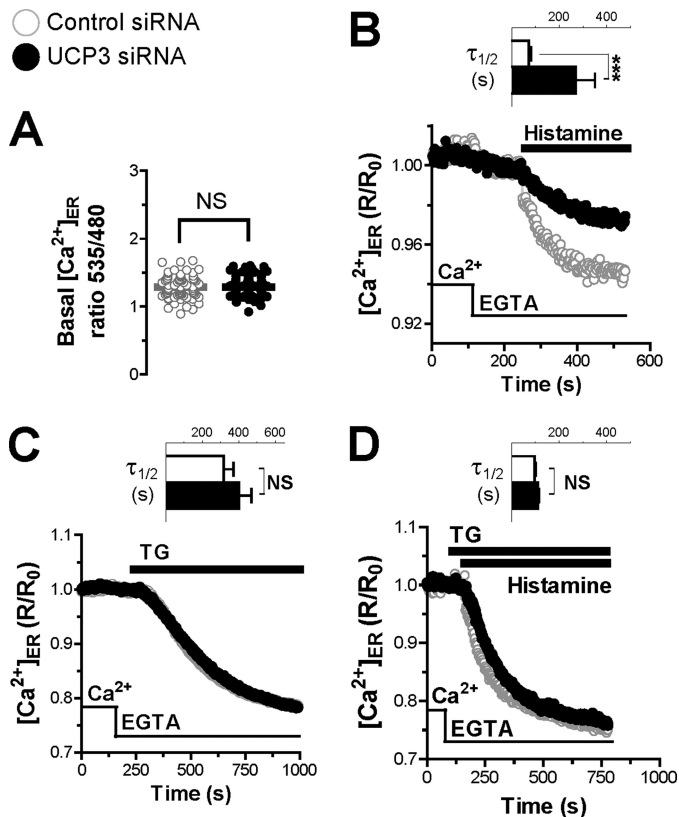
FIGURE 3. **Effect of UCP3 knockdown on ER Ca²⁺ release.** HeLa cells were transiently co-transfected with the ER Ca²⁺ probe D1$_{ER}$ and with the Ctrl (scramble) siRNA or the UCP3 siRNA for 48 h and washed, and Ca²⁺ responses were measured. *A*, resting D1$_{ER}$ ratio values of 73 ($n = 8$) and 77 ($n = 8$) cells, transfected with Ctrl and UCP3 siRNA, respectively. *NS*, not stimulated. *B*, averaged [Ca²⁺]$_{ER}$ recordings of HeLa cells stimulated with 100 μM histamine in Ca²⁺-free medium and related statistical evaluation (*inset*) of the UCP3 siRNA effects on the kinetics of Ca²⁺ release. For the latter statistics, the D1$_{ER}$ responses were fitted with a one-phase exponential decay function to extract the half-time. *Bars* are mean ± S.E. of 73 ($n = 8$) and 77 cells ($n = 8$) for Ctrl and UCP3 siRNA, respectively. ***, $p < 0.001$. *C*, the same as in *B*, but stimulating the cells with 1 μM TG. *Bars* are mean ± S.E. of 69 ($n = 8$) and 74 cells ($n = 9$) for Ctrl and UCP3 siRNA, respectively. *D*, the same as in *B*, but preincubating the cells with 1 μM TG 40 s before histamine stimulation. *Bars* are mean ± S.E. of 59 ($n = 5$) and 54 cells ($n = 5$) for Ctrl and UCP3 siRNA, respectively.

FIGURE 4. **Effect of UCP3 knockdown on ER Ca²⁺ refilling in intact and permeabilized cells.** *A*, SERCA2 immunoblot of HeLa cells transfected with Ctrl or UCP3 siRNA for 48 h. 50 μg/lane of protein from cell extracts was analyzed, using actin as loading control. *B, left*, averaged [Ca²⁺]$_{ER}$ recordings of intact HeLa cells during ER Ca²⁺ refilling. After 15 μM BHQ induced Ca²⁺ release in Ca²⁺-free medium, cells were washed, and Ca²⁺ was then added to assess the kinetics of store refilling. Data were fitted with the sigmoidal equation to extract the EC$_{50}$ (*right*), and they are mean ± S.E. of 40 ($n = 5$) and 30 cells ($n = 4$) for Ctrl and UCP3 siRNA, respectively. **, $p < 0.01$. *C, left*, averaged [Ca²⁺]$_{ER}$ recordings during ER Ca²⁺ release and refilling in permeabilized cells. The K⁺-rich intracellular buffer was supplemented with 1 mM Mg-ATP and 1 mM MgCl$_2$ to allow ER Ca²⁺ refilling. Where indicated, 100 μM digitonin (*dig*), 15 μM BHQ, and 100 nM free Ca²⁺ were added. *Right*, statistical evaluation of the ER Ca²⁺ refilling kinetics. EC$_{50}$ was determined as described for *B*. Data are mean ± S.E. of 47 ($n = 3$) and 33 cells ($n = 3$) for Ctrl and UCP3 siRNA, respectively. *NS*, not stimulated.

"Discussion" to compare our results with recent data of the Graier group (37)). The restoration of normal ER Ca²⁺ release in cells depleted of UCP3 by SERCA inhibitors suggested that the activity of SERCA was increased in these cells. The expression levels of SERCA2b assessed by Western blot (Fig. 4*A*) and real-time quantitative PCR (not shown) were not influenced by UCP3 depletion. To directly estimate the activity of SERCA, intact cells were transiently treated with the reversible inhibitor BHQ to deplete ER Ca²⁺ stores, and Ca²⁺ was then readmitted to promote store refilling. As shown in Fig. 4*B*, the kinetics of ER refilling were faster in cells depleted of UCP3, the time required to reach half-maximal refilling being increased by 14 s, confirming that SERCA pumps were more active in these cells. This difference was not observed in permeabilized cells, however, the kinetics of ER refilling being identical in this condition (Fig. 4*C*). Our [Ca²⁺]$_{ER}$ measurements thus indicate that the activity of SERCA pumps is increased in intact cells depleted of UCP3.

Effect of SERCA Inhibition on Mitochondrial Ca²⁺ Uptake in UCP3-depleted Cells—The effects of SERCA inhibitors on [Ca²⁺]$_{ER}$ handling prompted us to investigate whether SERCA

inhibition could normalize mitochondrial Ca²⁺ uptake in cells depleted of UCP3. To test this possibility, we measured the [Ca²⁺]$_{mit}$ responses evoked by Ca²⁺ release and by Ca²⁺ influx in cells treated with TG. As shown in Fig. 5*A*, the [Ca²⁺]$_{mit}$ responses evoked by Ca²⁺ release from stores and by SOCE were identical in control and UCP3-depleted cells treated with the SERCA inhibitor. Parallel [Ca²⁺]$_{cyto}$ measurements confirmed that both the release and the influx components were normal in UCP3-depleted cells treated with TG (supplemental Fig. S6), whereas the SOCE component remained blunted after washout of the reversible SERCA inhibitor BHQ (supplemental Fig. S7). These results confirm that UCP3 modulates cellular Ca²⁺ signals by interfering with the activity of SERCA.

To verify that UCP3 depletion did not alter mitochondrial Ca²⁺ uptake, we measured [Ca²⁺]$_{mit}$ responses evoked by the addition of Ca²⁺ to permeabilized cells. As shown in Fig. 5*B*, the addition of 3.5 μM free Ca²⁺ to permeabilized cells evoked robust [Ca²⁺]$_{mit}$ elevations that were observed irrespective of the depletion of UCP3. The [Ca²⁺]$_{mit}$ elevations were prevented by the MCU-inhibitor Ru360 both in control and in UCP3-depleted cells, and the Ru360-sensitive mitochondrial Ca²⁺ uptake was not significantly different between the two conditions (Fig. 5*B, right panel*). These data indicate that UCP3 does not contribute to mitochondrial Ca²⁺ uptake.

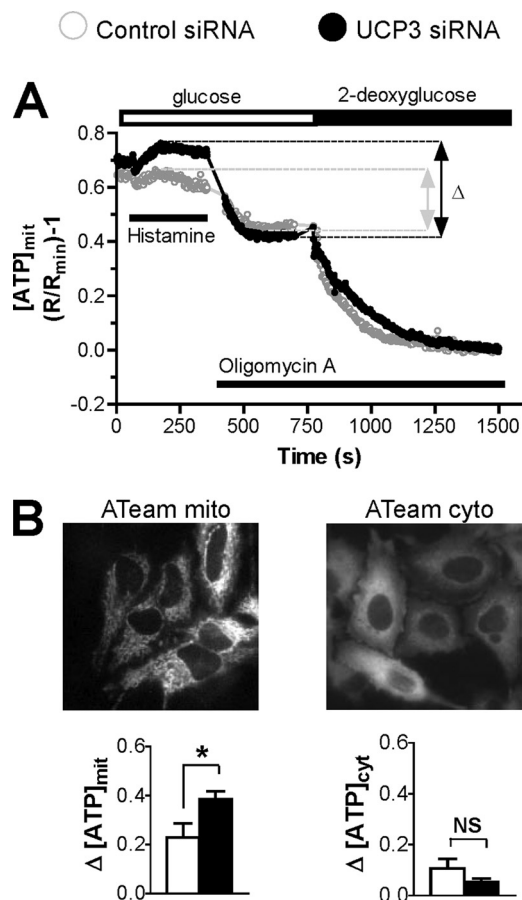*Effect of UCP3 Depletion on Mitochondrial ATP Production*—Because UCPs have been proposed to uncouple oxidative phos-
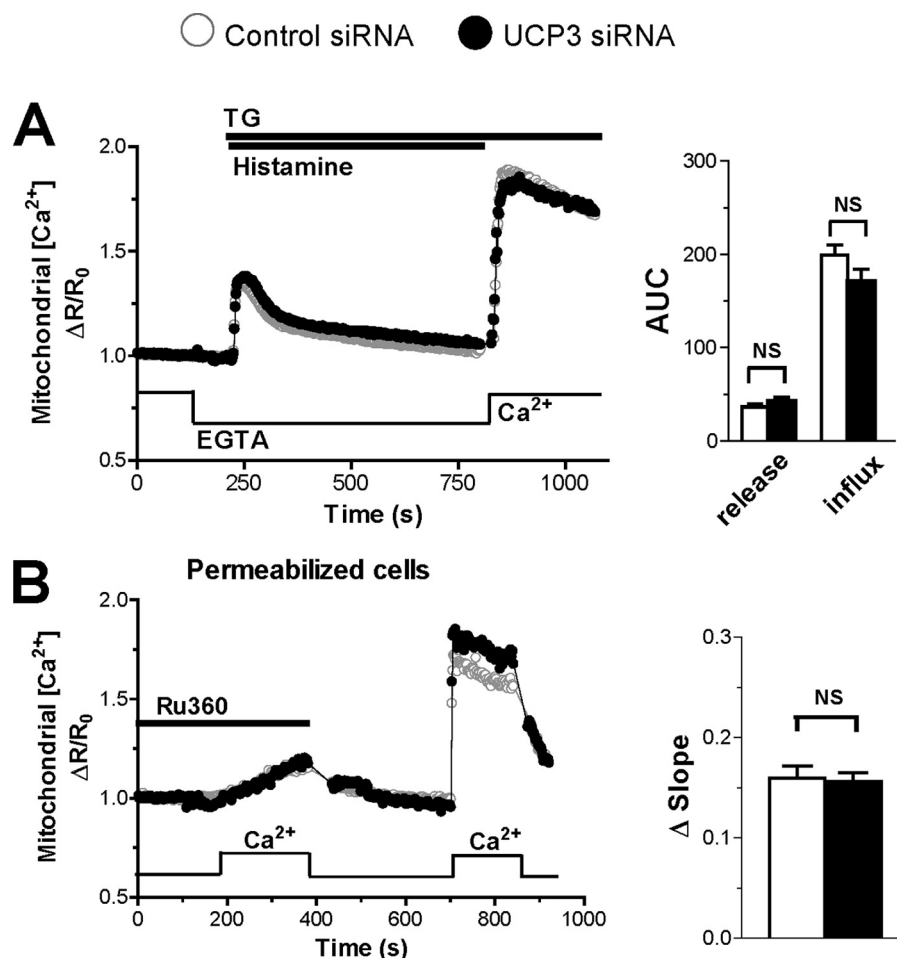
FIGURE 5. **Effect of SERCA inhibition or cell permeabilization on mitochondrial Ca²⁺ elevation.** *A*, the same protocols and conditions as in Fig. 2 were used to deplete Ca^{2+} stores and to monitor Ca^{2+} release and then the influx component in mitochondria, but in the presence of the SERCA pump inhibitor 1 μM TG. Histamine was 100 μM. *Left*, average of $[Ca^{2+}]_{mit}$ recordings from Ctrl (scramble) siRNA or the UCP3 siRNA cells. *Right*, statistical evaluation of the UCP3 knockdown on the integrated $[Ca^{2+}]_{mit}$ responses evoked by histamine or after Ca^{2+} readmission, from data shown in the *left panel. Bars* are mean $\pm$ S.E. of 51 ($n = 5$) and 45 cells ($n = 4$) for Ctrl and UCP3 siRNA, respectively. *NS*, not stimulated. *AUC*, area under the curve. *B*, Ru360-sensitive mitochondrial Ca^{2+}-uptake in permeabilized cells, in ATP-depleted medium. HeLa cells were transiently co-transfected with the mitochondrial calcium probe 4mtD3cpv and the indicated siRNAs. After permeabilization with digitonin, $[Ca^{2+}]_{mit}$ was measured in intracellular buffer. *Left*, original $[Ca^{2+}]_{mit}$ recordings of permeabilized HeLa cells during the addition of 3.5 μM free Ca^{2+} in the presence of or after wash-out of the mitochondrial Ca^{2+} uniporter inhibitor Ru360 (10 μM). *Right*, statistical evaluation of UCP3 siRNA effects on the slope of Ca^{2+} elevation. For the latter statistics, the Ca^{2+} responses for each trace were fitted with a linear function, and the Ru360-dependent slope was subtracted from the following one in the absence of the inhibitor. *Bars* are mean $\pm$ S.E. of 79 ($n = 6$) and 67 ($n = 6$) cells for Ctrl and UCP3 siRNA, respectively.

phorylation from ATP production, we postulated that mitochondria could generate more ATP at low UCP3 levels, thereby favoring the activity of nearby SERCA. Such a local control of SERCA pumps by mitochondrial ATP production was previously proposed (40), and the interaction between SERCA and mitochondria was postulated from the local competition between SERCA and mitochondria for the uptake of Ca^{2+} (41). To test whether mitochondria produced more ATP in UCP3-depleted cells, we prevented mitochondrial ATP production by inhibiting the ATP synthase with oligomycin or the respiratory chain with antimycin A and measured the $[Ca^{2+}]_{cyto}$ influx component evoked by readmission of Ca^{2+} to cells stimulated with agonists, as in Fig. 2*A*. We used this experimental paradigm as agonist-evoked Ca^{2+} entry was the component most sensitive to UCP3 depletion. Unfortunately, inhibition of mitochondrial ATP production severely decreased agonist-evoked Ca^{2+} entry, an effect that had been previously reported (38). Interestingly, the effects of UCP3 depletion disappeared in the presence of the inhibitors (supplemental Fig. S8), consistent with a role of mitochondrial ATP production in the alterations in Ca^{2+} handling.

To confirm that the effects of UCP3 depletion are mediated by the availability of ATP, we measured changes in ATP levels occurring in individual living cells with the genetically encoded ATP-sensitive probes ATeam (33). These FRET-based probes were efficiently targeted to the cytosol and the mitochondrial matrix (Fig. 6*B*), enabling real-time monitoring of changes in $[ATP]_{cyt}$ and $[ATP]_{mit}$ by ratiometric measurements. As shown in Fig. 6*A*, basal $[ATP]_{mit}$ levels were slightly elevated in cells depleted of UCP3 and increased further following exposure to histamine (*filled circles*). In contrast, the addition of histamine had little effect on $[ATP]_{mit}$ in control cells (*open circles*). We then sequentially added oligomycin and 2-deoxyglucose to assess the contribution of the mitochondrial ATP synthase and of glycolysis to the $[ATP]_{mit}$ and $[ATP]_{cyt}$ signal. Oligomycin had a relatively modest effect on $[ATP]_{cyt}$ levels, indicating that

FIGURE 6. **Effect of UCP3 knockdown on mitochondrial and cytosolic [ATP].** HeLa cells were transiently transfected with the mitochondrial or the cytosolic ATP probes ATeam$_{mito}$ or ATeam$_{cyto}$, respectively, together with the indicated siRNA for 48 h. *A*, averaged [ATP]$_{mit}$ changes elicited by 100 μM histamine and inhibition of mitochondrial ATP synthesis with oligomycin A (10 μg/ml) in cells perfused with 10 mM glucose as metabolic substrate and after inhibition of glycolysis with 10 mM 2-deoxyglucose. *B, upper panels*, mitochondrial (*left*) and cytosolic (*right*) ATeam signals recorded at 535 nm. *Left lower panel*, statistical evaluation of the histamine-induced, oligomycin A-sensitive [ATP]$_{mit}$ changes. *Bars* are mean $\pm$ S.E. of $n = 4$ (44 cells) and $n = 5$ (59 cells) for Ctrl and UCP3 siRNA, respectively. *Right lower panel*, statistical evaluation of the histamine-induced, oligomycin A-sensitive [ATP]$_{cyt}$ changes. *Bars* are mean $\pm$ S.E. of $n = 5$ (60 cells) and $n = 5$ (64 cells) for Ctrl and UCP3 siRNA, respectively. [ATP]$_{cyt}$ changes were recorded by applying the same protocol as in *A*. *, $p < 0.05$. *NS*, not stimulated.

most of the cytosolic ATP is of glycolytic origin in HeLa cells, consistent with the earlier ATeam study (33). In contrast, oligomycin significantly decreased [ATP]$_{mit}$ levels (Fig. 6*A*), indicating that the activity of the ATP synthase was detectable with the mitochondrial probe. Strikingly, the amplitude of the oligomycin-sensitive [ATP]$_{mit}$ component was nearly doubled in UCP3-depleted cells (Fig. 6*B, bottom left panel*). This effect was only observed with the mitochondria-targeted probe and not with the cytosolic probe (Fig. 6*B, bottom right panel*). The residual [ATP]$_{mit}$ levels of control and UCP3-depleted cells treated with oligomycin were similar and decreased with identical kinetics upon the addition of 2-deoxyglucose, indicating that the glycolytic activity was not affected by UCP3 depletion. The higher mitochondrial ATP concentration observed in UCP3-depleted cells stimulated with histamine therefore likely reflected the higher activity of the ATP synthase in these cells and indicates that mitochondria produce more ATP in cells

depleted of UCP3. ATeam measurements in cells overexpressing UCP3 revealed that these cells produced less mitochondrial ATP (supplemental Fig. S2*C*), confirming the inverse correlation between UCP3 levels and mitochondrial ATP production.

DISCUSSION

There has been some confusion lately as to the identity of the long sought after Ca^{2+} uniporter of mitochondria because three distinct families of proteins were proposed to contribute to mitochondrial Ca^{2+} uptake: UCP2 and UCP3 (37), Letm1 (10), and MICU1 (12). MICU1 is a single-pass transmembrane protein unlikely to form a pore that has been proposed to modulate Ca^{2+} uniport activity (12). Letm1 was shown to catalyze electrogenic 1:1 Ca^{2+}/H+ exchange, but this contradicts earlier studies showing that Letm1 drives electroneutral K$^+$/H+ exchange (8, 42). The claim that UCP2 and UCP3 contribute to mitochondrial Ca^{2+} uptake was disputed early on because mice lacking the UCP2 and UCP3 isoforms have robust uniporter activity (7). In follow-up studies, UCPs were shown to facilitate the mitochondrial uptake of the Ca^{2+} released from the ER, but not of the Ca^{2+} entering across SOCE channels (37). Here, we show that UCP3 does not contribute to mitochondrial Ca^{2+} uptake but indirectly alters cellular Ca^{2+} homeostasis by modulating mitochondrial ATP production. Our data show that UCP3 silencing boosts mitochondrial ATP production and enhances the Ca^{2+} pumping activity of SERCA. The ensuing alteration of cellular Ca^{2+} handling mimics reduced mitochondrial Ca^{2+} uptake.

Consistent with the original finding of Trenker *et al.* (6), we observed that UCP3 depletion reduced [Ca^{2+}]$_{mit}$ elevations evoked by histamine in intact cells, an effect most pronounced in Ca^{2+}-containing medium (Figs. 1 and 2). However, this phenotype was not due to reduced uniport activity because UCP3 depletion did not reduce [Ca^{2+}]$_{mit}$ signals in permeabilized cells and in cells treated with inhibitors of SERCA pumps or of mitochondrial ATP production (Figs. 5 and 6). Instead, UCP3 depletion was associated with decreased Ca^{2+} entry (Figs. 1*B* and 2*A*), blunted ER Ca^{2+} depletion (Fig. 3*B*), and increased mitochondrial ATP production (Fig. 6). The cytosolic and ER calcium defects also disappeared in cells treated with SERCA inhibitors (Figs. 3 and 5). These observations indicate that UCP3 does not mediate mitochondrial Ca^{2+} uptake but has a global effect on cellular Ca^{2+} homeostasis that requires functional SERCA and normal mitochondrial ATP production.

These data clarify the role of UCP3 in Ca^{2+} homeostasis and confirm several earlier observations, notably 1) the reduced [Ca^{2+}]$_{mit}$ elevations in UCP3-depleted cells exposed to agonists (Fig. 2*C* of Ref. 43), Fig. 1*C* of Ref. 44, and Fig. 2*A* of Ref. 37); and 2) the lack of UCP3 effects on [Ca^{2+}]$_{mit}$ elevations evoked by Ca^{2+} readmission to cells with inhibited SERCA (Figs. 2*B* and 3*B* of Ref. 37). These observations were interpreted as evidence that UCP3 is required for mitochondrial Ca^{2+} uptake during the rapid release of Ca^{2+} from ER stores, but not during the slow entry of Ca^{2+} across SOCE channels. Our simpler interpretation is that the effects of UCP3 depletion in intact cells are due to alterations in the rates of SERCA pumping because the differences disappear entirely in cells treated with SERCA inhibitors. Thus, in intact cells, the mito-

chondrial Ca^{2+} uptake rates indeed correlate with the expression levels of UCP2/3, as reported previously (6), but this effect is indirect and mediated by SERCA.

The requirement for active SERCA appears at odds with the blunted $[Ca^{2+}]_{mit}$ responses reported in cells co-stimulated with histamine and the SERCA inhibitor BHQ (Figs. 2*A*, 3*A*, and 4*A* of Ref. 37). However, our data show that effective SERCA inhibition requires at least 30 s of preincubation with TG and that BHQ releases Ca^{2+} more slowly than TG (supplemental Fig. S3). Thus, SERCA pumps were likely not fully inhibited in these experiments, and the UCP3 effects could still reflect alterations in the rates of SERCA pumping. Our data from permeabilized cells also diverge from the data of Trenker *et al.* 6, who reported a reduced Ca^{2+} uptake in isolated liver mitochondria from $UCP2^{-/-}$ mice (Fig. 3 of Ref. 6). In our hands, the Ru360-sensitive component of mitochondrial Ca^{2+} uptake was not affected by UCP3 depletion in permeabilized HeLa cells (Fig. 5*B*). These data are consistent with the normal mitochondrial Ca^{2+} uptake reported by Brookes *et al.* (7) in purified heart and liver mitochondria treated with UCP inhibitors and in skeletal muscle mitochondria isolated from $UCP2^{-/-}$ and $UCP3^{-/-}$ mice (Figs. 1 and 2 of Ref. 44). To account for these discrepancies, Trenker *et al.* (44) argued that the failure of Brookes *et al.* (7) to detect UCP3 effects in permeabilized cells was due to the harsher conditions of their purification procedure that used differential centrifugation instead of density gradients. Size distribution analysis revealed that mitochondria isolated by density gradient had a larger diameter (0.75/1.00 μm *versus* 0.25/0.50 μm for differential centrifugation, supplemental Fig. S1 of Ref. 44). This increase in mitochondrial size could reflect a different amount of mitochondria-associated ER membranes, ER-derived structures that co-purify with mitochondria during isolation (45). Mitochondria-associated ER membranes are enriched in ERp57, a protein that directly interacts with SERCA2b and modulates its activity (46). The presence of functional SERCAs on mitochondria-associated ER membranes co-purified with mitochondria isolated by density gradient might explain the effects of UCP2 ablation in this mitochondrial preparation. Finally, another discrepancy is the normal rates of SERCA pumping reported in cells overexpressing UCP2 or UCP3 in the original study by Trenker *et al.* (6) (supplemental Fig. S1*g* of Ref. 9) and in a more recent publication (Fig. 2*C* of Ref. 37). In our study, increased SERCA pumping was evident in cells depleted of UCP3 (Fig. 4*A*), and the rates of $[Ca^{2+}]_{ER}$ decrease were severely reduced during histamine stimulation (Fig. 3*B*). The increased activity of SERCA can account for the reduced influx of Ca^{2+} observed in cells depleted of UCP3 and treated with agonists (Fig. 2*A*), a phenotype that was not reported previously. Trenker *et al.* (6) did not attempt to measure $[Ca^{2+}]_{ER}$ changes in cells depleted of UCP2 or UCP3; thus, our data cannot be readily compared with theirs. However, based on the effects of UCP3 depletion, we would predict that UCP3 overexpression would decrease SERCA pumping.

Several mechanisms could explain the sensitivity of SERCA to changes in UCP3 levels. First, mitochondria could produce more reactive oxygen species in response to UCP3 depletion because an increase in UCP3 levels is known to lower reactive

oxygen species production (47). Because increased reactive oxygen species levels decrease SERCA activity, however (48, 49), UCP3 knockdown should decrease, rather than increase, SERCA activity. Alterations in reactive oxygen species levels are thus unlikely to account for the UCP3 effects that we report here. Second, UCP3 depletion could increase the number of ER-mitochondria contact sites or reduce the distance between mitochondria and the ER, enabling mitochondria to supply more ATP to nearby SERCA. Increased ER-mitochondria contact, however, should increase, rather than decrease, the efficiency of ER-mitochondria Ca^{2+} transmission. Finally, mitochondria could produce more ATP at low UCP3 levels, thereby fueling the activity of SERCA more efficiently. Our data indicate that this last mechanism is likely to occur because 1) the mitochondrial ATP production, measured with a genetically encoded ATP-sensitive indicator, was significantly increased following stimulation of cells with Ca^{2+}-mobilizing agonists; and 2) the UCP3 effects disappeared in cells treated with inhibitors of mitochondrial respiration and of the ATP synthase. UCP2/3 are mitochondrial inner membrane proteins whose first postulated function is to uncouple oxidative phosphorylation from ATP production (20). Although this uncoupling function is also disputed (16), the simplest explanation for the increased production of mitochondrial ATP observed in UCP3-depleted cells is that the energy stored in the proton-motive force is used more efficiently by the ATP synthase. Thus, a mild uncoupling function of UCP3 could account for the whole phenotype that we report here in UCP3-depleted cells, including 1) the increased production of mitochondrial ATP, 2) increased activity of SERCA, 3) decreased store-operated Ca^{2+} entry (due to reduced store Ca^{2+} depletion), and finally, 4) reduced mitochondrial Ca^{2+} uptake due to sequestration of the released Ca^{2+} by SERCA and (predominantly) to the blunted SOCE.

Our data highlight the pitfalls of interpreting alterations in $[Ca^{2+}]_{mit}$ signals occurring in intact cells. In intact cells, mitochondria are embedded in the ER, and the changes in matrix $[Ca^{2+}]$ are influenced by the activity of numerous Ca^{2+} transport proteins, including Ca^{2+} release and influx channels (InsP3R, Orai), Ca^{2+} pumps (SERCA, secretory pathway Ca^{2+}-ATPase (SPCA), and plasma membrane Ca^{2+}-ATPase (PMCA)), and Ca^{2+} buffering proteins, which are often overlooked. The simplistic interpretation that a reduced mitochondrial Ca^{2+} signal is due to reduced mitochondrial Ca^{2+} uptake disregards the complexity of the Ca^{2+} signaling circuitry in intact cells, where Ca^{2+} release and influx occur concomitantly with Ca^{2+} uptake catalyzed by SERCA and Ca^{2+} extrusion catalyzed by plasma membrane Ca^{2+}-ATPase. Our data show that a phenotype typical of defective mitochondrial Ca^{2+} uptake can in fact be explained by a metabolic alteration that changes the activity of Ca^{2+} pumps.

Note Added in Proof—A protein with all characteristic features of the Ca^{2+} uniporter of mitochondria was recently identified by two inde-

pendent groups (50, 51). The purified MCU protein exhibited Ca^{2+} channel activity in lipid bilayers (50), confirming that UCPs are not essential for mitochondrial Ca^{2+} uptake. The effects of UCPs on mitochondrial Ca^{2+} handling that were previously reported therefore likely reflect the metabolic alterations described in this study.

REFERENCES

1. Szabadkai, G., and Duchen, M. R. (2008) *Physiology* **23,** 84–94
2. Rimessi, A., Giorgi, C., Pinton, P., and Rizzuto, R. (2008) *Biochim. Biophys. Acta* **1777,** 808–816
3. Demaurex, N., Poburko, D., and Frieden, M. (2009) *Biochim. Biophys. Acta* **1787,** 1383–1394
4. Bernardi, P. (1999) *Physiol. Rev.* **79,** 1127–1155
5. Kirichok, Y., Krapivinsky, G., and Clapham, D. E. (2004) *Nature* **427,** 360–364
6. Trenker, M., Malli, R., Fertschai, I., Levak-Frank, S., and Graier, W. F. (2007) *Nat. Cell Biol.* **9,** 445–452
7. Brookes, P. S., Parker, N., Buckingham, J. A., Vidal-Puig, A., Halestrap, A. P., Gunter, T. E., Nicholls, D. G., Bernardi, P., Lemasters, J. J., and Brand, M. D. (2008) *Nat. Cell Biol.* **10,** 1235–1237; author reply 1237–1240
8. Nowikovsky, K., Froschauer, E. M., Zsurka, G., Samaj, J., Reipert, S., Kolisek, M., Wiesenberger, G., and Schweyen, R. J. (2004) *J. Biol. Chem.* **279,** 30307–30315
9. Dimmer, K. S., Navoni, F., Casarin, A., Trevisson, E., Endele, S., Winterpacht, A., Salviati, L., and Scorrano, L. (2008) *Hum. Mol. Genet.* **17,** 201–214
10. Jiang, D., Zhao, L., and Clapham, D. E. (2009) *Science* **326,** 144–147
11. Endele, S., Fuhry, M., Pak, S. J., Zabel, B. U., and Winterpacht, A. (1999) *Genomics* **60,** 218–225
12. Perocchi, F., Gohil, V. M., Girgis, H. S., Bao, X. R., McCombs, J. E., Palmer, A. E., and Mootha, V. K. (2010) *Nature* **467,** 291–296
13. Hajnóczky, G., and Csordás, G. (2010) *Curr. Biol.* **20,** R888–891
14. Palty, R., Silverman, W. F., Hershfinkel, M., Caporale, T., Sensi, S. L., Parnis, J., Nolte, C., Fishman, D., Shoshan-Barmatz, V., Herrmann, S., Khananshvili, D., and Sekler, I. (2010) *Proc. Natl. Acad. Sci. U.S.A.* **107,** 436–441
15. Da Cruz, S., De Marchi, U., Frieden, M., Parone, P. A., Martinou, J. C., and Demaurex, N. (2010) *Cell Calcium* **47,** 11–18
16. Azzu, V., and Brand, M. D. (2010) *Trends Biochem. Sci.* **35,** 298–307
17. Cannon, B., and Nedergaard, J. (2004) *Physiol. Rev.* **84,** 277–359
18. Cadenas, S., Echtay, K. S., Harper, J. A., Jekabsons, M. B., Buckingham, J. A., Grau, E., Abuin, A., Chapman, H., Clapham, J. C., and Brand, M. D. (2002) *J. Biol. Chem.* **277,** 2773–2778
19. Couplan, E., del Mar Gonzalez-Barroso, M., Alves-Guerra, M. C., Ricquier, D., Goubern, M., and Bouillaud, F. (2002) *J. Biol. Chem.* **277,** 26268–26275
20. Krauss, S., Zhang, C. Y., and Lowell, B. B. (2005) *Nat. Rev. Mol. Cell Biol.* **6,** 248–261
21. Chan, C. B., MacDonald, P. E., Saleh, M. C., Johns, D. C., Marbàn, E., and Wheeler, M. B. (1999) *Diabetes* **48,** 1482–1486
22. Himms-Hagen, J., and Harper, M. E. (2001) *Exp. Biol. Med.* (*Maywood*) **226,** 78–84
23. Goglia, F., and Skulachev, V. P. (2003) *FASEB J.* **17,** 1585–1591
24. Echtay, K. S., Esteves, T. C., Pakay, J. L., Jekabsons, M. B., Lambert, A. J.,

25. Portero-Otín, M., Pamplona, R., Vidal-Puig, A. J., Wang, S., Roebuck, S. J., and Brand, M. D. (2003) *EMBO J.* **22,** 4103–4110
25. Brand, M. D., and Esteves, T. C. (2005) *Cell Metab.* **2,** 85–93
26. Cioffi, F., Senese, R., de Lange, P., Goglia, F., Lanni, A., and Lombardi, A. (2009) *Biofactors* **35,** 417–428
27. Bézaire, V., Seifert, E. L., and Harper, M. E. (2007) *FASEB J.* **21,** 312–324
28. Arsenijevic, D., Onuma, H., Pecqueur, C., Raimbault, S., Manning, B. S., Miroux, B., Couplan, E., Alves-Guerra, M. C., Goubern, M., Surwit, R., Bouillaud, F., Richard, D., Collins, S., and Ricquier, D. (2000) *Nat. Genet.* **26,** 435–439
29. Brand, M. D., Affourtit, C., Esteves, T. C., Green, K., Lambert, A. J., Miwa, S., Pakay, J. L., and Parker, N. (2004) *Free Radic. Biol. Med.* **37,** 755–767
30. Nagai, T., Yamada, S., Tominaga, T., Ichikawa, M., and Miyawaki, A. (2004) *Proc. Natl. Acad. Sci. U.S.A.* **101,** 10554–10559
31. Palmer, A. E., Giacomello, M., Kortemme, T., Hires, S. A., Lev-Ram, V., Baker, D., and Tsien, R. Y. (2006) *Chem. Biol.* **13,** 521–530
32. Palmer, A. E., Jin, C., Reed, J. C., and Tsien, R. Y. (2004) *Proc. Natl. Acad. Sci. U.S.A.* **101,** 17404–17409
33. Imamura, H., Nhat, K. P., Togawa, H., Saito, K., Iino, R., Kato-Yamada, Y., Nagai, T., and Noji, H. (2009) *Proc. Natl. Acad. Sci. U.S.A.* **106,** 15651–15656
34. Jousset, H., Malli, R., Girardin, N., Graier, W. F., Demaurex, N., and Frieden, M. (2008) *Cell Calcium* **43,** 83–94
35. De Marchi, U., Campello, S., Szabò, I., Tombola, F., Martinou, J. C., and Zoratti, M. (2004) *J. Biol. Chem.* **279,** 37415–37422
36. Poburko, D., Liao, C. H., van Breemen, C., and Demaurex, N. (2009) *Circ. Res.* **104,** 104–112
37. Waldeck-Weiermair, M., Malli, R., Naghdi, S., Trenker, M., Kahn, M. J., and Graier, W. F. (2010) *Cell Calcium* **47,** 433–440
38. Frieden, M., James, D., Castelbou, C., Danckaert, A., Martinou, J. C., and Demaurex, N. (2004) *J. Biol. Chem.* **279,** 22704–22714
39. Prakriya, M. (2009) *Immunol. Rev.* **231,** 88–98
40. Landolfi, B., Curci, S., Debellis, L., Pozzan, T., and Hofer, A. M. (1998) *J. Cell Biol.* **142,** 1235–1243
41. Csordás, G., and Hajnóczky, G. (2001) *Cell Calcium* **29,** 249–262
42. Zotova, L., Aleschko, M., Sponder, G., Baumgartner, R., Reipert, S., Prinz, M., Schweyen, R. J., and Nowikovsky, K. (2010) *J. Biol. Chem.* **285,** 14399–14414
43. Waldeck-Weiermair, M., Duan, X., Naghdi, S., Khan, M. J., Trenker, M., Malli, R., and Graier, W. F. (2010) *Cell Calcium* **48,** 288–301
44. Trenker, M., Fertschai, I., Malli, R., and Graier, W. F. (2008) *Nat. Cell Biol.* **10,** 1237–1240
45. Hayashi, T., Rizzuto, R., Hajnoczky, G., and Su, T. P. (2009) *Trends Cell Biol.* **19,** 81–88
46. Li, Y., and Camacho, P. (2004) *J. Cell Biol.* **164,** 35–46
47. Toime, L. J., and Brand, M. D. (2010) *Free Radic. Biol. Med.* **49,** 606–611
48. Rosado, J. A., Redondo, P. C., Salido, G. M., and Pariente, J. A. (2006) *Mini Rev. Med. Chem.* **6,** 409–415
49. Ermak, G., and Davies, K. J. (2002) *Mol. Immunol.* **38,** 713–721
50. De Stefani, D., Raffaello, A., Teardo, E., Szabo, I., and Rizzuto, R. (2011) *Nature*, in press
51. Baughman, J. M., Perocchi, F., Girgis, H. S., Plovanich, M., Belcher-Timme, C. A., Sancak, Y., Bao, X. R., Strittmatter, L., Goldberger, O., Bogorad, R. L., Koteliansky, V., and Mootha, V. K. (2011) *Nature*, in press